J. Basic. Appl. Sci. Res., 3(4)716-728, 2013
© 2013, TextRoad Publication

ISSN 2090-4304
Journal of Basic and Applied Scientific Research
www.textroad.com

The Study of the Numerical Solution of Annular Quette Flow Problems by Using Various DVMs: Modified Implementation DVMs

Hedayat Fathi, Hassan Zeytoonian

Department of Science and Engineering, Islamic Azad University, Marivan Branch, Marivan, Iran

ABSTRACT

The problem of conservation and entropy for rarefied axisymmetric flows is investigated on the basis of Boltzmann - BGK equation. In this study, the elimination of shortcomings of Luc Mieussens' definitions for numerical velocity derivative is presented. For BGK equation, the implementation of Trigonometric Upwind Conservative (T-UCE), Trigonometric Central Conservative (T-CCE), Upwind Conservative (UCE) and Central Conservative (CCE) definitions has been tailored in such a way to satisfy many of conservation laws and dissipation of entropy. The problem of annular Couette flow of a rarefied gas with evaporation and condensation at boundary is resolved. In this review, it is found that the number of angular steps in the velocity space is a determining factor in satisfying conservation laws and dissipation of entropy law. As the size of the angular steps approaches zero, the results obtained through various definitions of the problem tend to improve. Moreover, the robustness of the modified implemented T-UCE numerical definition as a fully conservative and entropic numeric scheme is studied for various rarefied gas flow regimes. Results showed the esteem of the improved T-UCE scheme as a numerical definition which satisfies conservation law and dissipation of entropy in various rarefied Couette flow regimes.

KEYWORDS: Boltzmann-BGK equation, T-UCE definition, T-CCE definition, UCE definition, CCE definition, angular steps**,** Knudsen number.

1. INTRODUCTION

Various Numerical methods are used for solving Partial differential equation in very fields of science. In this paper we use a new numerical method for solving BGK equation [1, 2, 3, 4, 5]. One of the simple models of Boltzmann equation is the BGK model, developed by Bathnagar-Groos-Krook [6].

$$\partial_t f + v\nabla_x f = C(M[f]). \qquad (1)$$

The main concern in numerical computation of BGK equation, (1), is to develop a conservative and entropic numerical method. There are three different stages to a numerical solution of BGK equation; velocity, space and time discretization. In the first stage a robust velocity discretization of BGK equation, collision operator and transport operator, is pursued.

Schemes of velocity discretization that are used for BGK equation are called DVM schemes (Discrete Velocity Model). One of the first who numerically investigated the Boltzmann equation is Bergers [7] whose method was utilized extensively by others.

In velocity discretization of BGK collision operator the main problem is approximating the Maxwellian distribution function. Previous authors [8, 9] used precise quadratures of Gauss-Hermite type for approximating of Maxwellian distribution. Despite the accuracy of their quadratures, these methods lack the properties of conservation and dissipation of entropy. In [15], Mieussens proposed a method based on an entropy minimization principle, which gives a conservative and entropic discrete BGK collision operator. In this article the authors used Mieussens′ discrete BGK collision operator.

The cylindrical description of BGK equation involves inertia terms that are velocity derivatives of the distribution function. Velocity discretization of the cylindrical coordinate form of BGK equation includes the velocity discretization of the collision operator and the transfer operator. Defining a DVM method, depends on the numerical method which is used to approximate the inertia term. Representing the inertia term with a numerical derivative, has always been a concern of the researchers. Bergers [7] approximated the inertia terms by a Maxwellian distribution derivative that is not valid for non-equilibrium flows. Because of direct numerical discretization of inertia terms in DVM as introduced by Sone [11, 12], or Larino and Ray [13], their DVM schemes did not satisfy conservation laws and dissipation of entropy. For example, Sone's definition for inertia term that was

***Corresponding Author:** Hedayat Fathi, Department of Science and Engineering, Islamic Azad University, Marivan Branch, Marivan, Iran.

used in his DVM, made his DVM not to be an entropic one. good numerical definitions of inertia term are given by Mieussens' DVM's.

for the first time, Mieussens compared all of the previous numerical definitions of the inertia term [14]. he improved some of previous numerical definitions shortcomings by using some Trigonometric correction. Despite of Mieussens' corrections, the numerical definitions of inertia term had some defects in satisfing conservation laws and dissipation of enropy.

The scientific contribution of this paper is improveing some of remained defections of intertia term definitions presented by Mieussens. The problem of annular Couette flow of a rarefied gas with evaporation and condensation at boundary is resolved. It is found as the number of the angular steps increases, the results obtained through various definitions of the problem tend to improve. The results of previous studied in [15] and [16] are represented. In addition, the esteem of mention claim is studied theorically and numerically for TUCE DVM at various rarefied regimes with differient Knudsen numbers.

The remainder of the paper was organized as follows: In section II, some scientific background of Boltzmann equation is mentioned, in section III, analytical proof of improving results by increacing the number of the angular steps is presented, finally in section IV, the problem geometry and interpretation of results are shown.

II. BGK Equation

By solving BGK equation, the mass distribution function of monoatomic molecules (f) with position $x=(x,\ y,\ z)$ and molecular velocity $\mathbf{v}=(v_x,\ v_y, v_z)$ can be computed.

$$\partial_t f + v\nabla_x f = \frac{1}{\tau}(M[f]-f). \qquad (2)$$

In equation (2), $M[f]$ is a Maxwellian distribution function that depends on molecular velocity (**v**) and macroscopic fluid quantities such as macroscopic velocity (**u**) and temperature (T). The Maxwellian distribution function is defined as follows;

$$M[f]=\exp(\alpha\cdot m),$$
$$\boldsymbol{\alpha}=\{\log\left(\frac{\rho}{(2\pi\ R\ T)^{1.5}}\right)-\frac{|\mathbf{u}|^2}{2R\ T},\ \frac{\mathbf{u}}{R\ T},\ \frac{-1}{R\ T}\}. \qquad (3)$$

For convenient, in this article the symbols that were presented by Mieussens in [14] are used, so the microscopic vector **m** that contains five components is defined by the following relation;

$$\mathbf{m}(\mathbf{v})=(1,\mathbf{v},\ \frac{1}{2}|\mathbf{v}|^2). \qquad (4)$$

The microscopic vector defines mass, momentum vector and kinetic energy per unit mass of particle. The relaxation time of BGK model in relation (2) is defined by;

$$\tau=\frac{T^{\delta-1}}{c\ \rho}. \qquad (5)$$

In relation (5) δ is the component of viscosity law of gas and it depends on the molecular interaction potential and type of gas. The constant c is determined from the following relation;

$$c=RT_{ref}{}^{\delta}/\mu_{ref}. \qquad (6)$$

In equation (6), μ_{ref} is the viscosity of the gas at the reference temperature. Macroscopic properties of gas can be calculated by relation (7),

$$\rho=\langle f\rangle,\ \rho u=\langle v f\rangle,\ \frac{1}{2}\rho|u|^2+\frac{3}{2}kT=\left\langle\frac{1}{2}f|v|^2\right\rangle, \qquad (7)$$

the sign $\langle g\rangle$ denotes an integral of any vector or scalar function g, over-velocity coordinate. A macroscopic vector relation can be defined similar to macroscopic relation (4) as;

$$\boldsymbol{\rho}(\mathbf{u})=(\rho,\rho\mathbf{u},E). \qquad (8)$$

The relation between definitions of microscopic and macroscopic vectors is rewritten as;

$$\boldsymbol{\rho} = \left\langle \mathbf{m}(\mathbf{v})\ f \right\rangle . \qquad (9)$$

It can be seen that M[f] in equation (2) is a unique solution of entropy minimization problem as pointed out in equation (10) by Mieussens [14].

$$H\big(M[f]\big) = \min\left\{ H[g],\ g \geq 0 \quad \text{s.t } \langle \mathbf{m}\, g \rangle = \boldsymbol{\rho} \right\}. \qquad (10)$$

CONSERVATION LAWS AND ENTROPY DISSIPATION IN AXISYMMETRIC FLOWS

The axisymmetric form of equation (2) is obtained as described below. Space variables are written in a cylindrical coordinates system. $(x, y, z) = (x,\ r\cos\varphi,\ r\sin\varphi)$, and to make use of the axial symmetry in space, radial and azimuthal velocities are defined by,

$$v_r = v_y \cos\varphi + v_z \sin\varphi ,$$
$$v_\varphi = -v_y \sin\varphi + v_z \cos\varphi .$$

The assumption of axial symmetry now reads,

$$\partial_\varphi f\ (t, x, r, \varphi, v_x, v_r, v_\varphi) = 0 .$$

By substituting the above relations in relation (2), symmetric form of the equation is obtained.

$$\partial_t f + v_x \partial_x f + v_r \partial_r f + \frac{v_\varphi^{\ 2}}{r} \partial_{v_r} f - \frac{v_r v_\varphi}{r} \partial_v\ f = C(f). \qquad (11)$$

The velocity derivative terms in equation (11) are inertia terms that appears because of local coordinate system. According to equation (11) the number of independent variable is four. The number of independent variable is reduced by specifying new variables as in Sone and Sugimoto [6, 7]. By inserting the new variables ζ and ω as defined by**;**

$(v_r,\ v_\varphi) = (\zeta\ \cos\ \omega, \zeta\ \sin\ \omega)$, into equation (11), it is simplified to the following form;

$$\partial_t f + v_x \partial_x f + \zeta\cos\omega\, \partial_r f - \frac{\zeta \sin\omega}{r} \partial_\omega f = C \qquad (12)$$

A complete conservation form of equation (12) can be obtained as follow,

$$\partial_t (rf) + v_x \partial_x (rf) + \zeta\cos\omega\, \partial_r (rf) - \zeta\, \partial_\omega (\sin\omega\, f) = r\, C(f). \qquad (13)$$

With new variables, equation (9) is rewritten as,

$$(\rho,\ \rho u_X,\ \rho u,\ \rho u_r, E) = \int \left(1, v_X, \zeta\sin\omega, \zeta\cos\omega, \frac{1}{2}(v_X)^2\right) f\ \zeta\ dv_X d\zeta \qquad (14)$$

Multiplying two sides of (13) by $\mathbf{m}(\mathbf{v})$ and using (14) and integrating with respect to velocity, the conservation laws and the dissipation of entropy can be reached,

$$\partial_t (r\rho) + \partial_x (r\rho u_x) + \partial_r (r\rho u_r) = 0 , \qquad (15a)$$

$$\partial_t(r\rho u_x) + \partial_x r(\rho u_x^{\,2} + \rho\theta_{xx}) + \partial_r r(\rho u_x u_r + \rho\theta_{xr}) = 0, \quad (15b)$$

$$\partial_t(r\rho u_r) + \partial_x r(\rho u_x u_r + \rho\theta_{xr}) + \partial_r r(\rho u_r^{\,2} + \rho\theta_{rr}) = \rho\theta_{rr}, \quad (15c)$$

$$\partial_t(rE) + \partial_x r(u_x E + \rho(\theta_{xx}\, u_x + \theta_{xr}\, u_r) + q_x) + \partial_r r(u_r E + \rho(\theta_{xr}\, u_x + \theta_{rr}\, u_r) + q_r) = 0, \quad (15d)$$

$$\partial_t(r\int f \log f\ \zeta\, dv_x d\zeta\ d\omega) + \partial_x r(\int v_x f \log f\ \zeta\, dv_x d\zeta + \partial_r r\int \zeta\cos\omega\, f \log f\ \zeta\, dv_x d\zeta\, d\omega \le 0. \quad (15e)$$

Relations (15a)- (15e) are macroscopic partial differential equations of conservation and dissipation of entropy. Sone and Sugimoto considered Euler set of equation for Couette flow between two concentric axial cylinders and didn't consider entropy relation.

The intermediate steps between (13) and (15c) are elucidated below. Multiplying both sides of (13) by $\zeta\cos\omega$ and by considering (14) we arrive at:

$$\zeta\cos\omega\,\partial_t rf + v_x\,\zeta\cos\omega\,\partial_x rf + \zeta\cos\omega\,\zeta\cos\omega\,\partial_r rf - \zeta\,\zeta\cos\omega\,\partial_\omega(\sin\omega\, f) = r\,C(f)\,\zeta\cos\omega.$$

Since the contribution of $C(f)$ is zero in the above equation, its comparison with (15c) states the contribution of ∂_ω must be

$$\int_0^{2\pi}\cos\omega\,\partial_\omega(\sin\omega\ f)\ d\omega = \int_0^{2\pi}\sin^2\omega\, f\ \ d\omega.$$

This constrain and other constrains mentioned by Mieussens [14] are reformulated as;

$$\int_0^{2\pi}(\sin\omega\, f)\ d\omega = 0, \quad (16a)$$

$$\int_0^{2\pi}\cos\omega\,\partial_\omega(\sin\omega\ f)\ d\omega = \int_0^{2\pi}\sin^2\omega\, f\ \ d\omega, \quad (16b)$$

$$\int_0^{2\pi}\partial_\omega(\sin\omega\, f)\log f\ d\omega \le \int_0^{2\pi}\cos\omega\, f\ d\omega, \quad (16c)$$

$$\partial_\omega(\sin\omega) = \cos\omega. \quad (16d)$$

The establishment of these relations can guarantee that we are within the entropic discrete velocity model. Equation (16a) underwrites conservation laws of mass, energy and momentum in x (axial) direction. Equation (16b) assures conservation of momentum in radial direction. Equation (16c) ensures the dissipation of entropy and equation (16d) secures uniform flow. The momentum equation in tangential direction is not mentioned here.

DISCRETIZATION ON VELOCITY SPACE

By inserting the solution of (10) in the discretized collision operator $C_\kappa(f)$ it will transform to a conservative and entropic form [14]. Then only the transport part of equation (13) needs to be considered. According to relations (16a) - (16d), the importance of the parameter ω is apparent for (13) to be conservative and entropic. Hence, we only consider discretization in the ω direction. Complete velocity discretization is addressed in [14]. First, we

discretize independent variable ω by series $\{\omega_q\}_{q=0}^{Q}$ in which $\omega \in [0, 2\pi]$ and f_q is approximated by $f(\omega_q)$. Let the symbol D be defined as a finite difference operator that approximates ∂_ω at least to the first order. Then the relations (16a) – (16d) and 13 can be expressed in terms of this operator;

$$\sum_{q=0}^{Q} D(\sin\omega_q\ f) = 0\ , \tag{17a}$$

$$\sum_{q=0}^{Q} \cos\omega_q\ D(\sin\omega\ f)_q = \sum_{q=0}^{Q} \sin^2\omega\ f\ , \tag{17b}$$

$$\sum_{q=0}^{Q} D(\sin\omega\ f)_q\ \log f \le \sum_{q=0}^{Q} \zeta\cos\omega\ f_q\ , \tag{17c}$$

$$D(\sin\omega)_q = \cos\omega_q\ , \tag{17d}$$

$$\partial_t(r\ f_q) + v_x\partial_x(r\ f_q) + \zeta\cos\omega_q\ \partial_r(r\ f_q) - \zeta\ D(\sin\omega\ f) = C_\kappa(f). \tag{18}$$

Then with a definition for the D operator that satisfies (17a) – (17e) and inserting it into (18), a conservative and entropic DVM equation is reached;

III. Analytic Proof

In this section we analytically prove the improvement of numerical results by increasing number of ω is increased. The analytical proof steps are as follow: I. Appling numerical definition of inertia term, II. Using the assumption of increasing number of ω is increased and using the sandwich lemma.

The radial momentum satisfying condition, equation (17b), was developed by Mieussens [14] in its discretized form;

$$\sum_{q=0}^{Q} \cos\omega_q\ D(\sin\omega\ f)_q = \sum_{q=0}^{Q} \sin^2\omega\ f\ , \tag{17b}$$

Where the definition of D, a finite difference operator that approximates ∂_ω at least to the first order, is:

$$D(\sin\omega\ f)_q = \frac{1}{2\sin\frac{\Delta\omega}{2}}[((\sin\omega_{q+1/2})^+ f_{q+1} + (\sin\omega_{q+1/2})^- f_q) - ((\sin\omega_{q-1/2})^+ f_q + (\sin\omega_{q-1/2})^- f_{q-1})], \tag{19a}$$

for T-UCE scheme, where,

$$a^{\pm} = \frac{(a \pm |a|)}{2},\quad \Delta\omega = \omega_{q+1} - \omega_q,$$

$$\sin(\omega_{q\pm1/2}) = \sin(\omega_q \pm \frac{\Delta\omega}{2}),$$

$$\cos(\omega_{q\pm1/2}) = \cos(\omega_q \pm \frac{\Delta\omega}{2}).$$

And a second order approximation of ∂_ω for T-CCE scheme,

$$D(\sin\omega f)_q = \frac{1}{2\sin\Delta\omega}[\sin\omega_{q+1} f_{q+1} - \sin\omega_{q-1} f_{q-1}]. \tag{19a}$$

It can be demonstrated that this criterion will be satisfied by Mieussens T-UCE scheme [14] if the number of ω nodes are adequately increased. Out of other DVM schemes also used by researchers, the T-CCE scheme is picked out due to complying with conservation laws. A comparison of both definitions is presented in table1.

Table 1 Properties of T-UCE and T-CCE schemes [14]

scheme	Con. $\rho, E, \rho u_\varphi$	Con. ρu_r	entropy
T-UCE	yes	no	yes
T-CCE	yes	yes	no

As it is seen, T-UCE scheme satisfies all the properties except the momentum in radial direction. By demonstrating that if the number of ω nodes is increased, T-UCE scheme will satisfy the constrain (17b) and since other constrains are proved by the T-UCE scheme itself (see table 1.), it completes the conservative and the entropic definitions.

Rewriting Mieussens' T-UCE definition for $D(\sin\omega\ f)$ in equation (17b) the following equation is obtained,

$$\sum \cos\omega_q \{\frac{1}{2\sin\frac{\Delta\omega}{2}}[((\sin\ \omega_{q+1/2})^+ f_{q+1} + (\sin\omega_{q+1/2})^-\ f_q) - ((\sin\omega_{q-1/2})^+ f_q + (\sin\omega_{q-1/2})^-\ f_{q-1})]\} = \sum \sin^2\omega_q\ f_q, \quad (20)$$

while,

$$\Sigma h_{q-1/2}\ \sin\omega_q = \Sigma\Big(((\sin\omega_{q-1/2})^+ f_q + (\sin\omega_{q-1/2})^- f_{q-1})\Big)\sin\omega_q. \quad (27)$$

$$a^\pm = \frac{(a \pm |a|)}{2},\ \ \Delta\omega = \omega_{q+1} - \omega_q,$$

$$\sin(\omega_{q\pm1/2}) = \sin(\omega_q \pm \frac{\Delta\omega}{2}), \quad (21)$$

$$\cos(\omega_{q\pm1/2}) = \cos(\omega_q \pm \frac{\Delta\omega}{2}).$$

Considering h (numerical flux) as,

$$h_{q+\frac{1}{2}} = \Big(((\sin\omega_{q+1/2})^+ f_{q+1} + (\sin\omega_{q+1/2})^-\ f_q)\Big). \quad (22)$$

Therefore relation (20) is simplified in the following manner,

$$\Sigma\cos\ (\omega_q)\frac{1}{2\sin(\frac{\Delta\omega}{2})}\Big(h_{q+1/2} - h_{q-1/2}\Big) = \Sigma\sin^2\omega_q\ f_q. \quad (23)$$

As the number of the ω nodes increases $\Delta\omega$ tends to zero, $\lim_{\omega\to\infty} \Delta\omega \to 0$. Hence,

$$\lim_{\Delta\omega\to0} \sin(\omega_{q\pm1/2}) \cong \sin(\omega_q)\ ,$$

and

$$\lim_{\Delta\omega\to0} \cos(\omega_{q\pm1/2}) \cong \cos(\omega_q).$$

By using these approximations and applying some mathematical manipulation on the left hand side of equation (23), it simplifies to,

$$\sum \left(\frac{1}{2\sin\left(\frac{\Delta\omega}{2}\right)} \left(h_{q+1/2} - h_{q-1/2}\right) \cos\omega_{q+1/2}\right.$$

$$\left. + \frac{h_{q-1/2}}{2\sin\left(\frac{\Delta\omega}{2}\right)} \left(\cos\omega_{q+1/2} - \cos\omega_{q-1/2}\right)\right) = \qquad (24)$$

$$\sum \frac{1}{2\sin\left(\frac{\Delta\omega}{2}\right)} \left(h_{q+1/2}\cos\omega_{q+1/2} - h_{q-1/2}\right.$$

$$\left.\cos\omega_{q-1/2}\right) + \sum h_{q-1/2}\sin\omega_q.$$

In as much as,

$$g_{q+1/2} = h_{q+1/2}\cos\omega_{q+1/2}, \qquad (25)$$

expression (24) is simplified to,

$$\sum \frac{1}{2\sin\left(\frac{\Delta\omega}{2}\right)} \left(g_{q+1/2} - g_{q-1/2}\right) + \sum h_{q-1/2}\sin\omega_q. \qquad (26)$$

Since the contribution of the first term of the expression (26) is zero, then by substituting $h_{q-1/2}$ from (22), into the expression (26), it becomes,

By increasing the number of nodes, ω, and use of sandwich lemma,

$$f_q \cong f_{q-1} \cong f_\xi, \quad q-1 \le \zeta \le q, \qquad (28)$$

the relation (27) is recasted to,

$$\sum \left(\left((\sin\omega_{q-1/2})^+ f_q + (\sin\omega_{q-1/2})^- f_{q-1} \right) \right) \sin\omega_q =$$

$$\sum \left(\left((\sin\omega_{q-1/2})^+ + (\sin\omega_{q-1/2})^- \right) \right) f_\zeta \sin\omega_q$$

$$= \sum \frac{\left(\sin\omega_{q-1/2} + \left|\sin\omega_{q-1/2}\right|\right) + \left(\sin\omega_{q-1/2} - \left|\sin\omega_{q-1/2}\right|\right)}{2}$$

$$f_\xi \sin\omega_q \cong \sum \sin\omega_q \; f_\xi \sin\omega_q = \sum f_q \sin^2\omega_q.$$

Hence, radial momentum equation is satisfied if the number of ω is increased. See reference [15].
So the properties of T-UCE definition in table 1 will change as follow:

Table (2) Properties of modified T-UCE

scheme	Con. $\rho, E, \rho u_\varphi$	Con. ρu_r	entropy
T-UCE	yes	yes	yes

The forms of CCE, UCE numeric definitions is presented in [14]. The properties of T-CCE, UCE and CCE DVM's are also represented in table 3.

Table (3) properties of different DVM's [14].

Scheme	Cons. ρU_r	Cons $\rho U_x, E, \rho$	Entropy
UCE	No	Yes	No
CCE	No	No	No
T - CCE	Yes	Yes	No

IV. PROBLEM'S GEOMETRY AND CONDITIONS

The problem of the Couette flow between two coaxial cylinders with unlimited length, on whose boundaries, evaporation and condensation take place, has been solved through four definitions (T-CCE, CCE, UCE, and T-UCE) representing the numerical derivative term. The radius of the outer and the inner cylinder is 2m and 1m, respectively. The pressure on he surface of the inner and the outer cylinder is 0.0708 and 0.0779 kPa respectively, and the surface temperature for each of them is assumed to be 300˚k [14]. The rotational velocities of the outer cylinder have been taken as 0, 53 and 105m/s. In circumstances which inner cylinder rotates, the velocity amount is 53m/s. Other Parameters are retained as in [14] (such as nodes of other microscopic velocities, number of points in radial direction and etc.).

Knudsen number is computed based on the inner cylinder radius as Sone, Sugimoto, Aoki and Takada did in [6, 7]. Results are calculated in on amounts 0.1, 1 and 10 of Knudsen number.

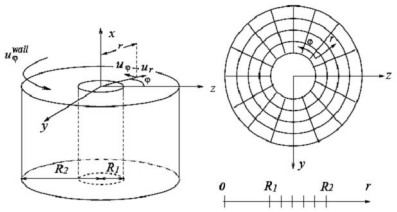

Problem's Geometry [14].

RESULTS

Result of Improved T - UCE Scheme

Analytical modification of T-UCE is tested numerically by increasing the number of ω - nodes. It was established by previous authors that T-CCE scheme delivers a conservative radial momentum [14]. It is why the new results from improved TUCE are compared with the result of TCCE scheme in this section.

Results in figures 2, 3 and 4 show the comparison of obtained radial velocity distributions with those of the T-CCE scheme. In figure 2, radial velocity distributions are calculated for a range of different velocities of the outer cylinder of which three velocities are depicted in figure 1, 0, 53 and 105 m/s. In figure 3, radial velocity distribution are obtained for two different Knudsen number (1 and 10) when outer cylinder rotate velocity is 53 m/s. In state that inner cylinder rotate velocity is 53 m/s and outer cylinder is at rest, the radial velocity distribution in two different Knudsen amounts 1 and 10 is presented in figure 4. As it is evident from this figures, there exists a very good agreement between the results of improved T - UCE scheme with T-CCE ones. It is evident Form figures 2, 3 and 4 that agreement is valid at various rarefied regime of Couette flow at various Knudsen number and various velocity of outer and inner cylinder.

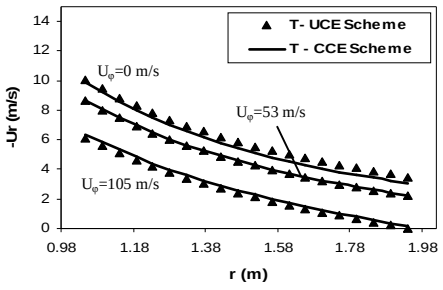

Figure 1. Comparison of radial velocity profile of modified T-UCE scheme with Corresponding one of T-CCE scheme (Kn=0.1, $U_{\varphi,\ outer}$=0, 53, 105 m/s) [15].

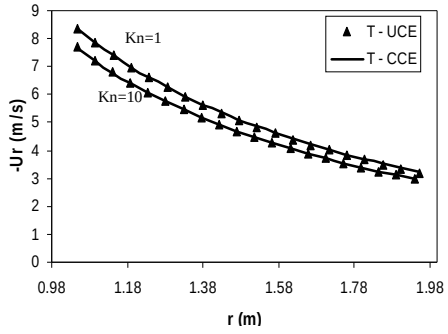

Figure 2. Comparison of radial velocity profile of modified T-UCE scheme with Corresponding one of T-CCE scheme (Kn=1, 10, $U_{\varphi,\ outer}$= 53 m/s).

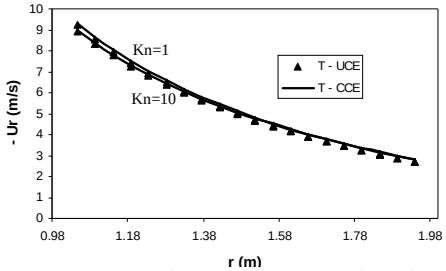

Figure 3. Comparison of radial velocity profile of modified T-UCE scheme With Corresponding one of T-CCE scheme (Kn=1, 10, $U_{\varphi,\ inner}$= 53 m/s).

According to figure 2 the amount of reverse radial velocity reduces as the velocity of outer cylinder increases. As it is shown in figures 2, 3 and 4, the radial velocity between two cylinders is negative; therefore, the direction of flow is from outer cylinder to inner cylinder. Figures 5, 6 and 7 clearly show the difference between the solutions of the two schemes as it was expected since T-CCE scheme does not abide by the dissipation entropy relation, see table 1. Its proof has given by Mieussens [14]. The kinetic entropy decrease, along the radial direction, is evident from T-UCE curves. The decrease of kinetic entropy in radial direction proves that the direction of radial velocity reverses in view of the fact that every process does not happen unless macroscopic entropy increases in the direction of the process.

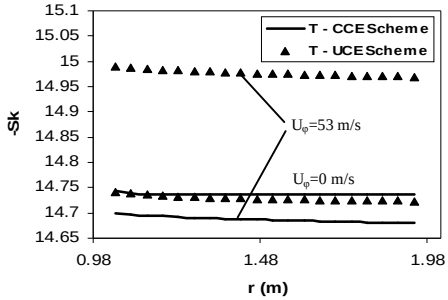

Figure 4. Kinetic entropy distributions for T-UCE and T-CCE schemes (Kn=0.1, $U_{\varphi,\ outer}$=0, 53 m/s) [15].

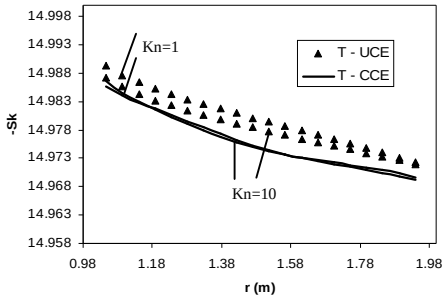

Figure 5. Kinetic entropy distributions for T-UCE and T-CCE schemes (Kn=1, 10, $U_{\varphi,\ outer}$= 53 m/s).

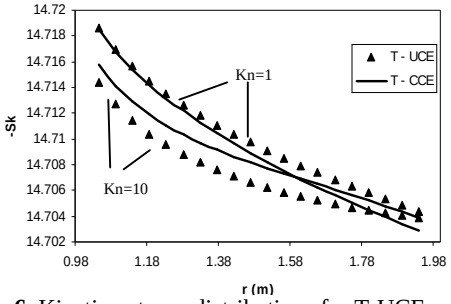

Figure 6. Kinetic entropy distributions for T-UCE and T-CCE schemes (Kn=1, 10, $U_{\varphi,\ inner}$= 53 m/s).

Since both DVM methods satisfy conservative mass, tangential momentum and energy equations, there exists a very good agreement between results of both schemes, see table 1. These are illustrated in figures 8 to 16. Tangential velocity distribution, temperature and density for two different tangential velocities are presented in Figures 8, 9 and 10. Figure 10 shows increase of the density of gas near the outer cylinder and decrease of the density near the inner cylinder with the increase in velocity of outer cylinder.

Figures 11 to 13 show the tangential velocity, temperature and density distribution at two different Knudsen numbers.

Figures 14 to 16 show respectively the tangential velocity, temperature and density curves at two different Knudsen number when inner cylinder velocity is 53 m/s.

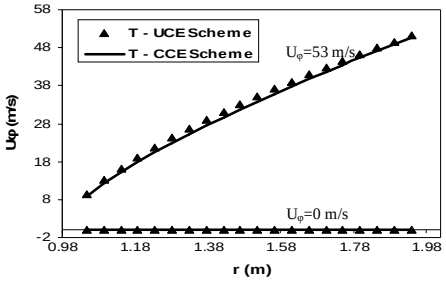

Figure 7. Tangential velocity distributions for T-UCE and T-CCE schemes (Kn=0.1, $U_{\varphi, outer}$=0, 53 m/s) [15].

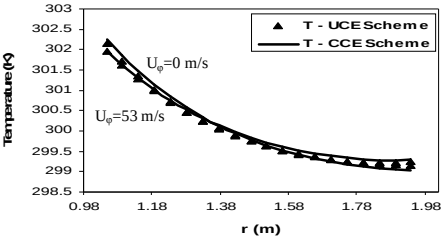

Figure 8. Temperature profiles for T-UCE and T-CCE schemes (Kn=0.1, $U_{\varphi, outer}$=0, 53 m/s, To=300k) [15].

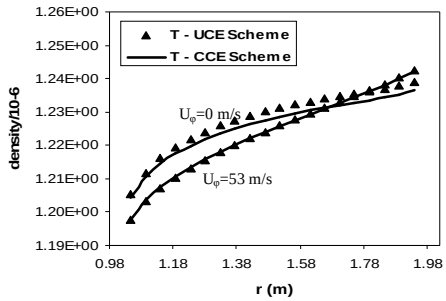

Figure 9. Density profiles for T-UCE and T-CCE schemes (Kn=0.1, $U_{\varphi, outer}$=0, 53 m/s) [15].

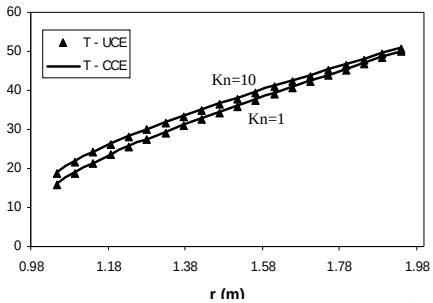

Figure 10. Tangential velocity distributions for T-UCE and T-CCE schemes (Kn=1, 10, $U_{\varphi, outer}$= 53 m/s).

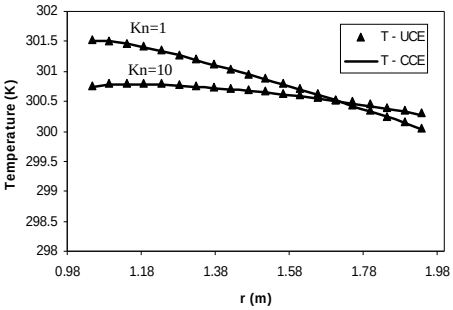

Figure 11. Temperature profiles for T-UCE and T-CCE schemes (Kn=1, 10, $U_{\varphi, outer}$= 53 m/s, To=300k).

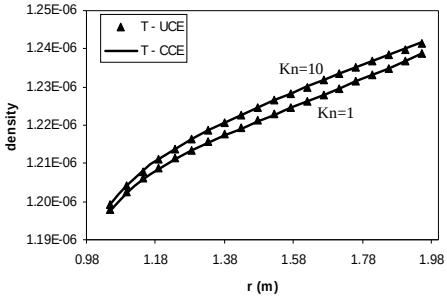

Figure 12. Density profiles for T-UCE and T-CCE schemes (Kn=1, 10, $U_{\varphi, outer}$= 53 m/s).

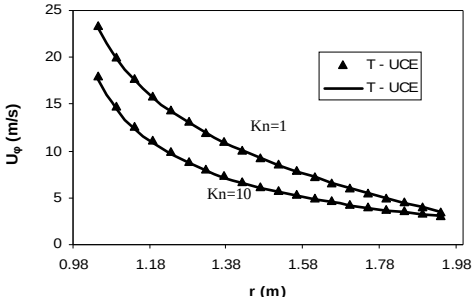

Figure 13. Tangential velocity distributions for T-UCE and T-CCE schemes (Kn=1, 10, $U_{\varphi, inner}$= 53 m/s).

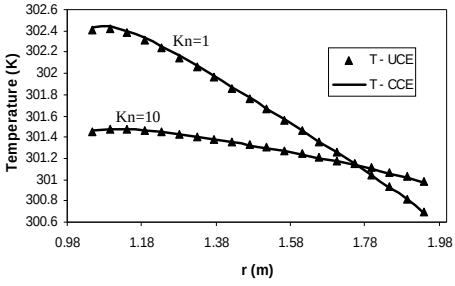

Figure 14. Temperature profiles for T-UCE and T-CCE schemes (Kn=1, 10, $U_{\varphi, inner}$= 53 m/s, To=300k).

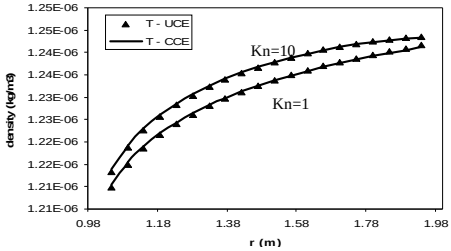

Figure 15. Density profiles for T-UCE and T-CCE Schemes (Kn=1, 10, $U_{\varphi, inner}$= 53 m/s).

According to Figures 17, 18 and 19, the pressure near the outer cylinder wall is greater than the pressure near the inner cylinder wall. This fact is in conformity with the results shown in figure 2, 3 and 4 since the flow direction is from the high to low pressure.

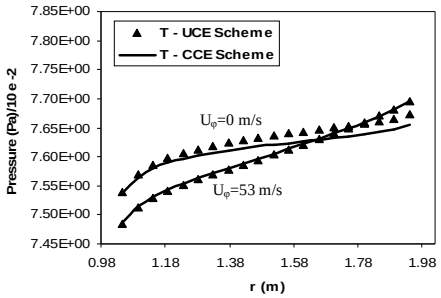

Figure 16. Comparison of pressure distribution of modified T-UCE scheme with corresponding one of T-CCE scheme (Kn=0.1, $U_{\varphi, outer}$=0, 53 m/s)

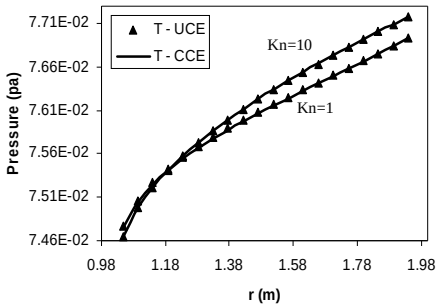

Figure 17. Comparison of pressure distribution of modified T-UCE scheme with corresponding one of T-CCE scheme (Kn=1, 10, $U_{\varphi, outer}$= 53 m/s).

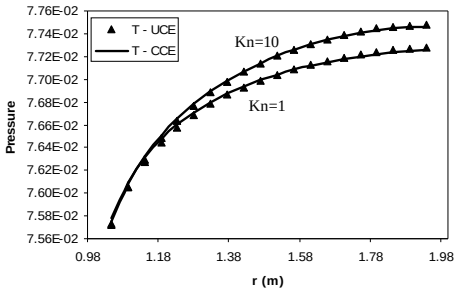

Figure18. Comparison of pressure distribution of modified T-UCE scheme with corresponding one of T-CCE scheme (Kn=1, 10, $U_{\varphi, inner}$= 53 m/s).

Results of Improved T - CCE, CCE and UCE Schems

In figure (20), radial velocity curves for the four definitions, CCE, UCE, T-UCE, and T-CCE, have been compared with each other. As can be seen from figure (20), three schemes of T-UCE, UCE, and CCE, which did not satisfy the momentum equation along the radius (table 2), by increasing the number of angular steps in the velocity space, are able to satisfy the equation of the conservation of radial momentum. Figures (21), (22), and (23), respectively show the curves related to the density, temperature, and the tangential velocity distribution between the two cylinders, resulting from different definitions with increasing numbers of angular steps. These figures show that, as the number of angular steps in the velocity space increases, all the various definitions, once again, satisfy the equations of conservation of mass, energy, and momentum along the axis. Figure (24) shows the comparison between the kinetic entropy distribution of the CCE, UCE, and T-CCE definitions and that of the T-UCE definition. As we can see from figure (24), by increasing the number of angular steps in the velocity space, none of T-CCE, UCE and CCE numerical definition changes to an entropic method of solution. Properties of different DVM's after increasing the number of angular steps in the velocity space is presented in table 4.

Table (4) properties of different DVM's after increasing the number of angular steps in the velocity space [16].

Scheme	Cons. ρU_r	Cons ρU_x, E, ρ	Entropy
UCE	Yes	Yes	**No**
T - UCE	Yes	Yes	**Yes**
CCE	Yes	Yes	**No**
T - CCE	**Yes**	**Yes**	**No**

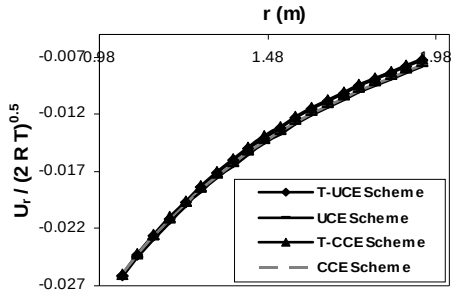

Figure 19. Comparison of the results of radial velocity distribution of the CCE, UCE and T-UCE definitions with those of the T-CCE definition (Kn=0.1, U_φ=53 m/s) [16].

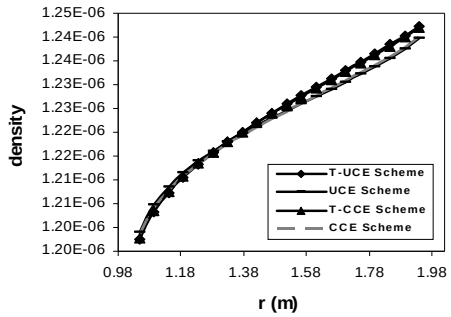

Figure 20. Comparison of the results of density distribution of the CCE, UCE and T-CCE definitions with those of the T-UCE definition (Kn=0.1, U_φ=53 m/s) [16].

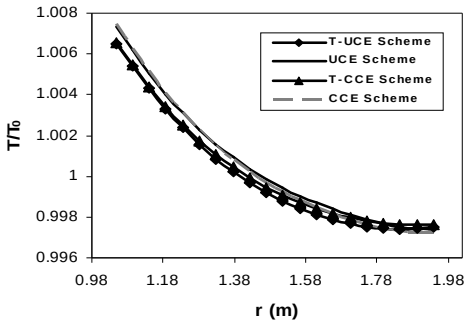

Figure 21. comparison of the results of temperature distribution of the CCE, UCE and T-CCE definitions with those of the T-UCE definition (T=300K, Kn=0.1, U_φ=53 m/s)[16].

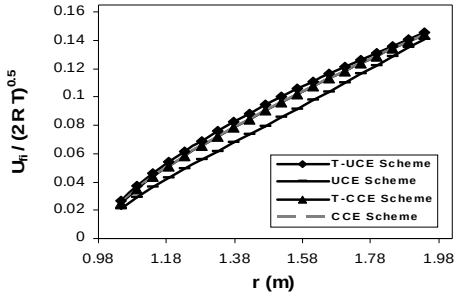

Figure 22. Comparison of the results of tangential velocity distribution of the CCE, UCE and T-CCE definitions with those of the T-UCE definition (Kn=0.1, U_φ=53 m/s) [16].

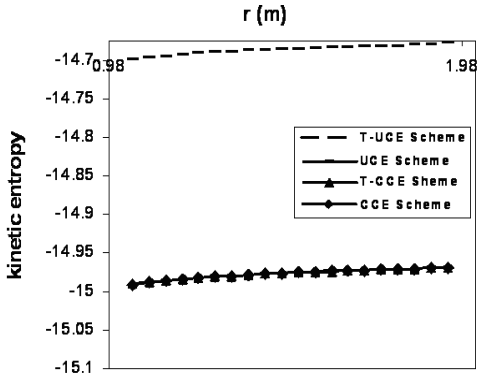

Figure 23. Comparison of the results of kinetic entropy distribution of the CCE, UCE and T-CCE definitions with those of the T-UCE definition (Kn=0.1, U_φ=53 m/s) [16].

Conclusion

It is clear from the results obtain for various numerical definition of inertia term that increasing the amount of angular node numbers causes the improving of numerical results and satisfying most of conversation laws. For example according to table 2 T-UCE numeric definition will satisfy all of conservation laws and other numerical definition will improve as table 4.

Acknowledgements

This work has been supported financially by Department of Engineering, Marivan Branch, Islamic Azad University, Marivan, Iran.

REFERENCES

1. Behrouz, R., 2010. Numerical Solutions of the Linear Volterra Integro-differential Equations. World Applied Sciences Journal. 7(12): 7-12.
2. Muhammad A. G., A. S. Arife, Majid Khan and I. Hussain, 2011. An Efficient Numerical Method for Solving Linear and Nonlinear Partial Differential. World Applied Sciences Journal, 14 (12): 1786-1791.
3. Fallah K., A. Fardad, N. Sedaghatizadeh, E. Fattahi and A. Ghaderi, 2011. Numerical Simulation of Flow around Two Rotating Circular Cylinders in Staggered Arrangement by Multi-Relaxation-Time Lattice Boltzmann Method. World Applied Sciences Journal 15 (4): 544-554.
4. Mohamad A. P., M. M. Shoshtari and A. Adib, 2011. Numerical Solution of Richards Equation by Using of Finite Volume Method. World Applied Sciences Journal 14 (12): 1838-1842.
5. Fatahi, B and F. Mehrdoust, 2010. Quasi Monte Carlo Algorithm for Computing Smallest and Largest Generalized Eigenvalue. World Applied Sciences Journal 9: 39-43.
6. Bathnagar, P. L., E. P. Gross and M. *A* Krook, 1954. A model for collision processes in gases. Journal of Physics Review, 1(94): 511-525.
7. Bergers, D., 1985, Kinetic model solution for axisymmetric flow by the method of discrete ordinates. Journal of Computational Physics, 2(57): 285-302.
8. Yang, J. Y and J. C. Hung, 1995. Rarefied flow computations using nonlinear model Boltzmann equations. Journal of Computational Physics, 2(120): 323–339.
9. Aoki, K., K. Kanaba and S. Takata, 1997. Numerical analysis of a supersonic rarefied gas flow past a flat plate. Journal Physics of Fluids, 9(4): 110-116.
10. Mieussens, L., 2000. Discrete velocity model and implicit scheme for the BGK equation of rarefied gas dynamics, Journal of Math. Models and meth. Appl.Sci. 8(10), 1121-1149.
11. Sone, Y., S. Takada and H. Sugimoto, 1996. The behavior of a gas in the continuum limit in the light of kinetic theory. Journal of Physics Fluids, 8(12): 3403-3413.
12. Sone, Y., H. Sugimoto and K. Aoki, 1998, Cylindrical Couette flows of a rarefied gas with evaporation and condensation: reversal and bifurcation of flows, Journal of Physics fluids, 11(2), 478-490.
13. Larina, I. N., and V.A. Rykov, 1998. A numerical method for calculating axisymmetric rarefied gas flows. Journal of Computational Mathematic, 38(8): 1391-1403.
14. Mieussens, L., 2000. Discrete-velocity models and numerical schemes for the Boltzmann-BGK equation in plane and axisymmetric geometries. Journal of Computational Physics. 2(162), 429-466.
15. Zeytoonian, H., R. Masah, S. Navardi, M. Mortezaei and M. Najafi, 2008. A numerical solution to annular Couette flow with evaporation and condensation. In the Proceeding of Sixth International Conference on Heat Transfer, Fluid Mechanic and Thermodynamics (HEFAT 2008), University of Pretoria, pp: 146-153.
16. Zeytoonian, H., R. Masah, S. Navardi, M. Mortezaei and M. Najafi, 2008. Improvement of results of different velocity discretization schemes for BGK equation. In the proceeding of the Seventh Annual International Conference of Iranian Aerospace society (Aero 2008), Sharif University of Technology, pp: 991-995. (in Persian)